

## Corrosion Effects on the Magnetic Behavior of Magnetic Circuit of an Induction Machine

M'hamed Ouadah<sup>1, \*</sup>, Omar Touhami<sup>2</sup>, Rachid Ibtouen<sup>2</sup>,  
Mohammed Khorchef<sup>3</sup>, and Djilali Allou<sup>3</sup>

**Abstract**—In This paper, the effect of corrosion on the magnetic behavior of a magnetic material used as a magnetic circuit in the induction machines is studied. With this objective, the magnetic properties of the samples with corrosion and without corrosion were evaluated by the study of hysteresis loops using a homemade vibrating sample magnetometer (VSM). The magnetic parameters extracted from the hysteresis loops such as saturation magnetization, coercive, remanent magnetization, squareness ratio, magnetic permeability, and hysteresis area were analyzed. It was shown that more energy is required to demagnetize the sample with corrosion than the sample without corrosion, and the hysteresis loss in the case of the sample with corrosion is more than the case of the sample without corrosion. These mean that when the corrosion is presented in the magnetic circuits of the induction machine, the hysteresis loss increases, consequentially reducing the machine efficiency.

### 1. INTRODUCTION

Induction machine efficiency is the measure of the ability of an induction machine to convert electrical energy to mechanical energy [1–5], i.e., watts of electric power are supplied to an induction machine at its electrical terminals, and the horsepower of mechanical energy is taken out of the induction machine at the rotating shaft. Therefore, the only power absorbed by the induction machine is the energy losses incurred in making the conversion from electrical to mechanical energy.

Energy losses incurred in making the conversion from electrical to mechanical energy can be separated into three categories (1) mechanical losses, (2) winding losses, and (3) iron losses [6–13].

Mechanical loss in the induction machines basically consists of bearing friction. Winding losses (often also called copper, ohmic, or resistive losses) are the losses created by the current in the windings of an induction machine. The energy loss in a magnetic material (iron loss) is a very significant characteristic in the energy efficiency of induction machines. This loss is termed magnetic loss. Traditionally, magnetic loss has been divided into two components: eddy current loss and hysteresis loss. Eddy current loss is created by the induced current in magnetic material, while hysteresis loss is due to the magnetic prosperities of a magnetic material used as a magnetic circuit in the induction machine. This loss is proportional to the area enclosed by a hysteresis loop.

Several factors can affect the magnetic behavior of magnetic materials [14–17], such as the chemical composition of materials, the heat treatment applied to the steel, and the grain size of the material (the larger the grain size is, the lower the hysteresis loss is). In [14], the authors studied the factors affecting magnetic properties of Fe-Si-AL and Ni-Fe-Mo alloys and showed that the addition of silicon increases the resistivity and reduces eddy current losses and coercivity of the alloy.

---

*Received 27 February 2018, Accepted 25 April 2018, Scheduled 7 May 2018*

\* Corresponding author: M'hamed Ouadah (ouadah@gmail.com).

<sup>1</sup> Ecole Supérieure en Sciences Appliquées à Alger, BP 474, Place des Martyrs Alger 16001, 1<sup>er</sup> Novembre, Algeria. <sup>2</sup> Laboratoire de Recherche en Electrotechnique, Ecole Nationale Polytechnique, 10, av. Pasteur El Harrach, Algiers, BP 182, 16200, Algeria.

<sup>3</sup> Research Center in Industrial Technologies CRTI, BP 64, route de Dely-Ibrahim, Chéraga, Algiers 16033, Algeria.

This paper diagnoses the effect of corrosion on the magnetic behavior of a magnetic material used as a magnetic circuit of the induction machine. To achieve this objective, the magnetic properties of the samples with and without corrosion were evaluated by the study of hysteresis loops using a homemade vibrating sample magnetometer (VSM). The measurements were taken with maximum applied magnetic field of 21.5 kOe at room temperature. The magnetic parameters extracted from the hysteresis loops namely saturation magnetization ( $M_s$ ), coercive field ( $H_c$ ), remanent magnetization ( $M_r$ ), squareness ratio  $M_r/M_s$ , relative permeability ( $\mu_r$ ), and hysteresis area were analyzed for all the samples. The results show that more energy is required to demagnetize the sample with corrosion than the sample without corrosion, and the hysteresis loss in the case of the sample with corrosion is more than the case of the sample without corrosion. These mean that when the corrosion is presented in the stator of the induction machine, hysteresis loss increases, and consequentially the efficiency of the induction machine will be reduced

## 2. MATERIAL AND METHODS

The samples with and without corrosion used in this study have been cut from a magnetic circuit of the induction machine as shown in Figure 1.

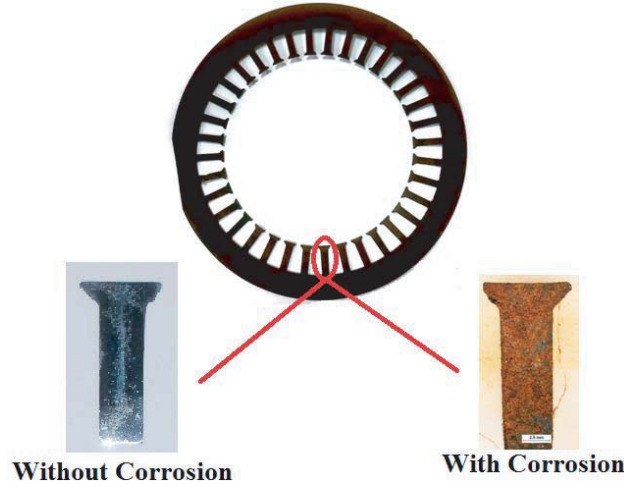


**Figure 1.** Magnetic circuit of an induction machine.

According to X-ray fluorescence (XRF) spectrometer measurements, the chemical composition of the magnetic material of magnetic circuits is presented in Table 1 (in wt.%).

**Table 1.** Chemical composition of the magnetic material used in induction machine.

Elements	Fe	Si	Cu	Mn	Al	S	Ni	Cr	Mo	V	Ti	W
(%)	ba	2.75	0.	0.17	0.12	0.09	0.09	0.06	0.03	0.02	0.01	0.01

## 3. VSM MEASUREMENTS

It is conventional to discuss the properties of ferromagnetic materials in terms of various parameters associated with the hysteresis loop curve of the material. The hysteresis loop contains important information about the magnetic properties of the samples. Characteristics include saturation magnetization ( $M_s$ ), coercive field ( $H_c$ ), remanent magnetization ( $M_r$ ), squareness ratio  $M_r/M_s$ , relative permeability ( $\mu_r$ ), and hysteresis area (hysteresis loss). In this study and as shown in Figure 2, the



**Figure 2.** Vibrating sample magnetometer (VSM).

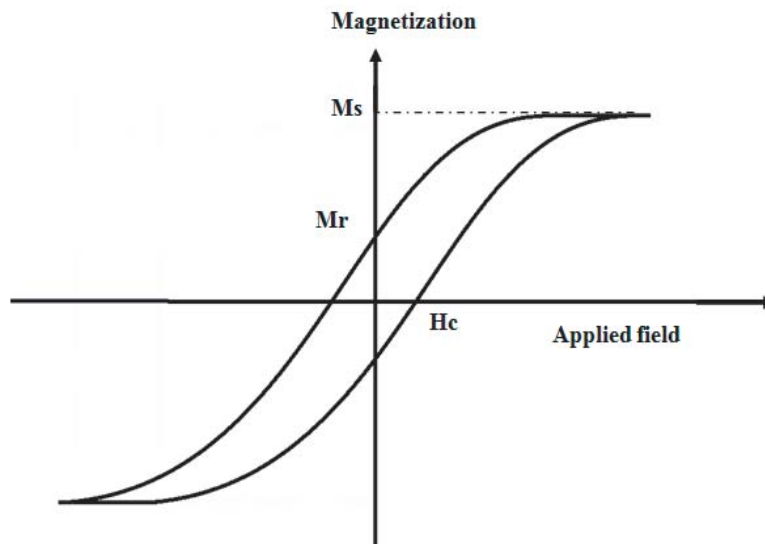


**Figure 3.** Typical form of a hysteresis loop.

magnetic proprieties of the samples are measured by a homemade vibrating sample magnetometer (VSM). Figure 3 shows such a typical form of a hysteresis loop, together with the definition of customary parameters.

When the material corrodes, an oxide layer (corrosion) will be formed. In order to show the effect of the corrosion layer on the magnetic behavior of the magnetic material used as a magnetic circuit in the induction machine, firstly, the magnetic properties of the samples with and without corrosion were evaluated by the study of hysteresis loops using VSM. Then, we removed the corrosion layer from the corroded sample in order to characterize the magnetic behavior. Figures 4(a), (b), (c) present different steps of characterization of the samples ((b) sample with corrosion, (c) sample without corrosion, and (d) the corrosion layer).

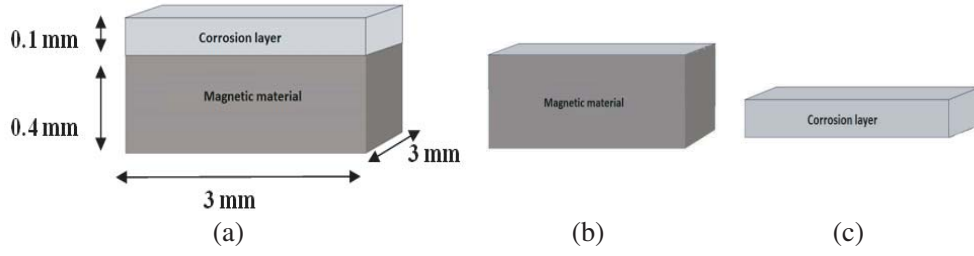


**Figure 4.** Steps of characterization, (a) sample with corrosion, (b) sample without corrosion and (c) corrosion layer.

#### 4. RESULTS AND DISCUSSION

The magnetic properties of the samples with and without corrosion of the magnetic material used as a magnetic circuit in the induction machines were characterized with a homemade Vibrating Sample Magnetometer (VSM). The measurements were taken with maximum applied magnetic field of 21.5 kOe at room temperature. Figure 5 shows magnetic hysteresis loops of the two samples. The magnetic parameters extracted from the hysteresis loops are summarized in Table 2, namely saturation magnetization ( $M_s$ ), coercive field ( $H_c$ ), remanent magnetization ( $M_r$ ), squareness ratio  $M_r/M_s$ , relative permeability ( $\mu_r$ ), and hysteresis area.

As shown in Figure 6, at the applied fields of 19352 kOe and 19.448 kOe, respectively, the samples with and without corrosion are fully saturated. Saturation magnetization ( $M_s$ ) was measured to be

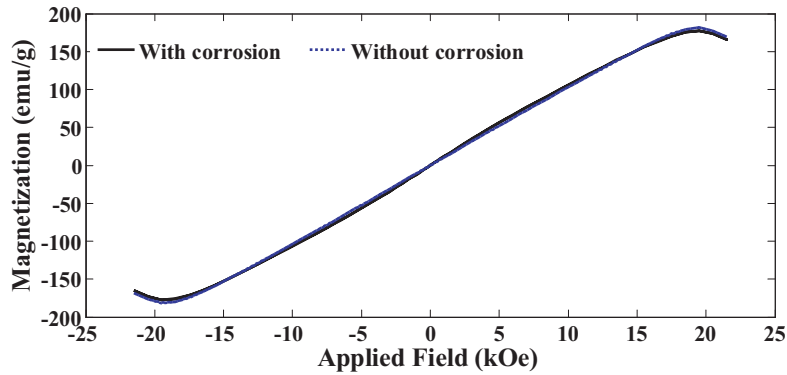


**Figure 5.** Hysteresis curves of the samples with and without corrosion, as obtained by VSM.

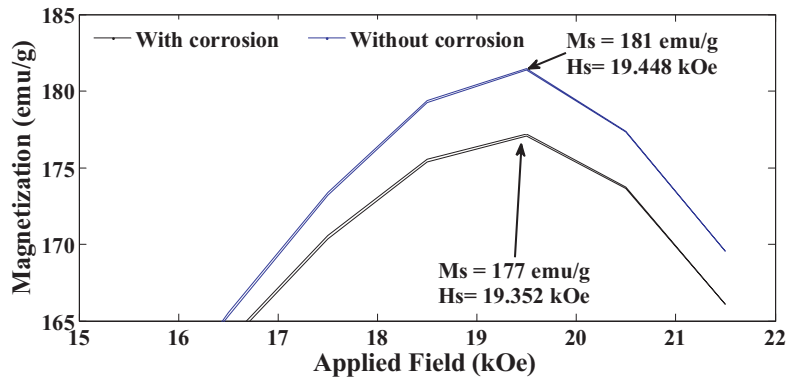


**Figure 6.** Zoom around the saturation magnetization for both the samples with and without corrosion.

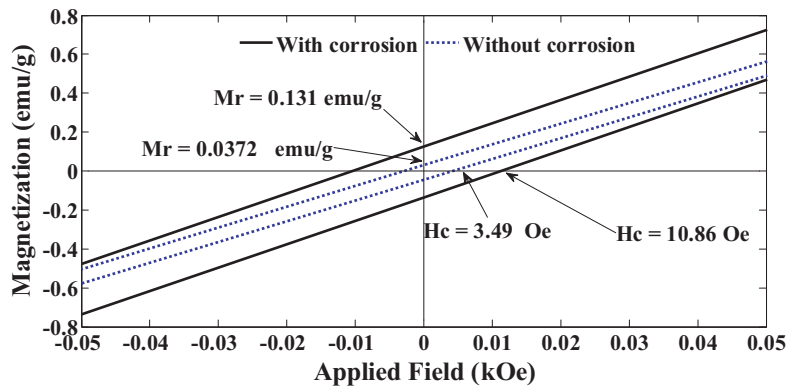


**Figure 7.** Zoom around the coercive field ( $H_c$ ) and the remanent magnetization ( $M_r$ ) for both the samples with and without corrosion.

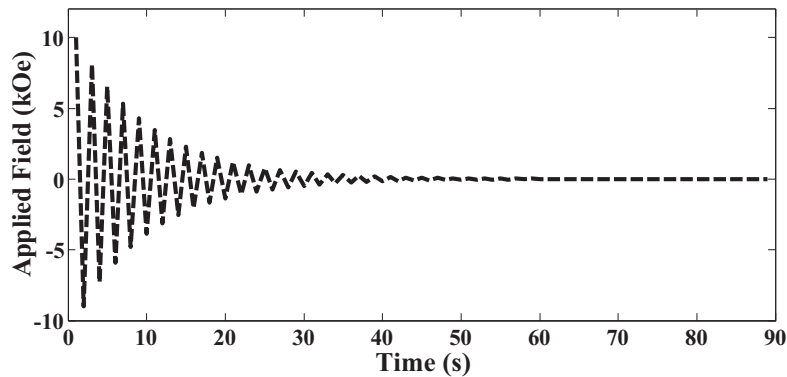


**Figure 8.** Applied demagnetized field of the samples with and without corrosion.

181 emu/g for the sample without corrosion and 177 emu/g for the sample with corrosion. In addition, as shown in Figure 7, the remanent magnetization ( $M_r$ ) values of the samples with and without corrosion are 0.131 emu/g and 0.0372 emu/g, respectively. The sample with corrosion showed a larger coercive field ( $H_c$ ) of 10.86 Oe than 3.49 Oe for the sample without corrosion.

This result indicates that more energy is required to demagnetize the sample with corrosion than the sample without corrosion. To justify this result, we demagnetize both the samples with and without corrosion. Figure 8 shows the applied demagnetized field of the samples with and without corrosion, and Figure 9 shows the variation of the magnetization for both the samples with and without corrosion as a function of the applied demagnetized field.

The squareness ratio, SQR ( $M_r/M_s$ ), were determined by the ratio of remanent magnetization to magnetization and recorded for both the samples with and without corrosion are 0.6 and 0.19 which are the measures of how square the hysteresis loops are. The relative permeability ( $\mu_r$ ) values of the samples with and without corrosion are 9634 and 8519, respectively. This indicates that the sample with corrosion is more permeable than the sample without corrosion.

The hysteresis loss of the material is present in the area enclosed by the hysteresis loop. Magnetic energy is in the loop area and is dissipated per unit volume if the material is completely cycled around one loop. The sample with corrosion showed a larger hysteresis loop of 7130 emu/g · Oe than 5450 emu/g · Oe for the sample without corrosion. This result indicates that, firstly, the sample with corrosion is magnetically hard compared to the sample with corrosion. Then the hysteresis loss in the case of the sample with corrosion is more than the sample without corrosion.

Figure 10 shows magnetic hysteresis loop of the corrosion layer. The magnetic parameters extracted from the hysteresis loop of the corrosion layer are summarized in Table 2. At the applied field of 7 kOe,

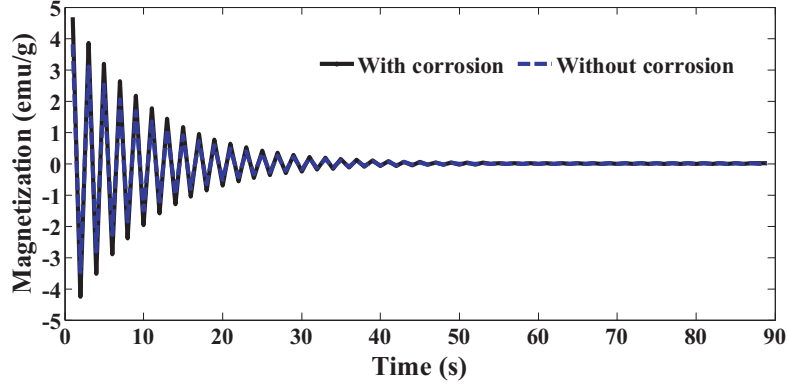


**Figure 9.** Magnetization as a function of the applied demagnetized field for the samples with and without corrosion.

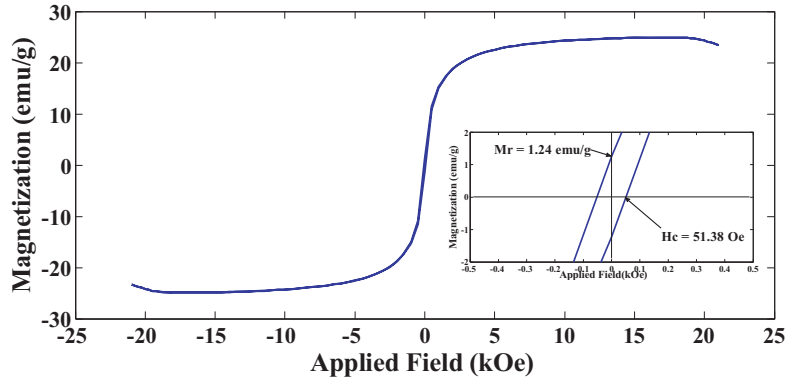


**Figure 10.** Hysteresis curve of the corrosion layer, as obtained by VSM.

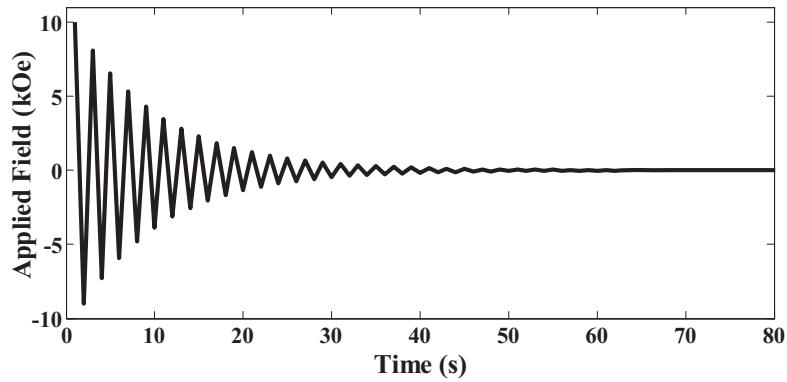


**Figure 11.** Applied demagnetized field of the corrosion layer.

the corrosion layer is fully saturated. Saturation magnetization ( $M_s$ ) was measured to be 24.9 emu/g. In addition, the corrosion layer showed a larger coercive field ( $H_c$ ) of 51.38 Oe. On the other hand, the remanent magnetization ( $M_r$ ) value is 1.24 emu/g. Figure 11 shows the demagnetized field in order to demagnetize the corrosion layer, and Figure 12 shows the variation of the magnetization of the corrosion layer as a function of the applied demagnetized field. It can be seen from this figure that the time of the demagnetization of the corrosion layer is greater than the time of the demagnetization for both the samples with and without corrosion. This result can also confirm that more energy is required to demagnetize the sample with corrosion than the sample without corrosion.

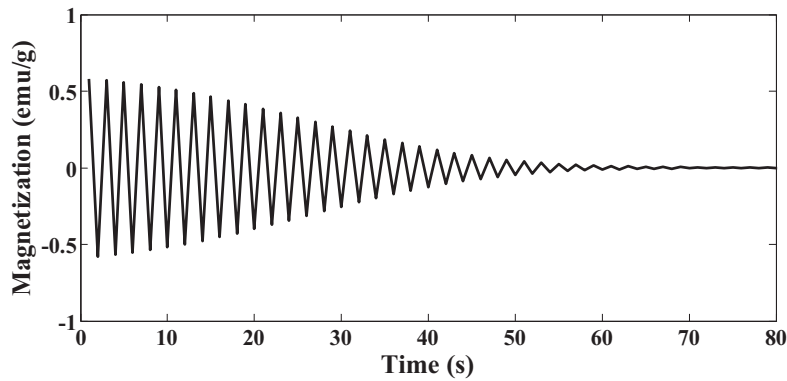


**Figure 12.** Magnetization as a function of the applied demagnetized field for the corrosion layer.

**Table 2.** Magnetic proprieties of the samples with corrosion, without corrosion and the corrosion layer.

Parameters	Samples	
	With corrosion	Without corrosion
Saturation magnetization (emu/g)	177	181
Saturation field (kOe)	19.352	19.448
Coercive field (Oe)	10.86	3.49
Remanent magnetization (emu/g)	0.131	0.0372
Squareness ratio ( $M_r/M_s$ )	0.060	0.019
Relative permeability	9634	8519
Hysteresis area (emu/g · Oe)	7130	5450

We can conclude that the presence of the corrosion layer on the magnetic material has a significant effect on the magnetic behavior of this material. The reduction in the magnetic characteristics of the sample with corrosion is due to the superposition of the two magnetic materials. The first one has high magnetic characteristic (magnetic material used as a magnetic circuit in the induction machine) superimposed by a magnetic material of a low magnetic characteristic (corrosion layer). This means that when the corrosion is presented in the stator of the induction machine, the hysteresis loss increases, and consequentially the efficiency of the induction machine will be reduced.

## 5. CONCLUSIONS

This paper diagnoses the effect of corrosion on the electromagnetic behavior of the magnetic material used as a magnetic circuit of the induction machines. The more important conclusions reached in this study are as follows:

- The presence of the corrosion layer on the magnetic materials used as a magnetic circuit has a significant effect on the magnetic behavior of these materials;
- More energy is required to demagnetize the sample with corrosion than the sample without corrosion;
- The hysteresis loss in the case of the sample is more than the case of the sample without corrosion;
- The presence of the layer corrosion on the magnetic circuit of the induction reduces the efficiency of this machine.

## APPENDIX A.

Technical parameters of homemade VSM.

Model	EZ 9 VSM
High accuracy	better than 1 mOe
Vibration frequency	75 Hz
Samples orientation	90°
Max applied field	22 kOe
Field noise as low as	5 mOe

## REFERENCES

1. Agamloh, E. B., "Induction motor efficiency," *IEEE Industry Applications Magazine*, Vol. 17, No. 6, 20–28, 2011.
2. Aminu, M., P. Barendse, and A. Khan, "Efficiency estimation of induction machines using nonintrusive no-load low voltage test," *2017 IEEE Energy Conversion Congress and Exposition (ECCE)*, 3171–3178, 2017.
3. Verucchi, C. J., R. Ruschetti, and G. Kazlauskas, "High efficiency electric motors: Economic and energy advantages," *IEEE Latin America Transactions*, Vol. 11, No. 6, 1325–1331, 2013.
4. Al-Badri, M. and P. Pillay, "Evaluation of measurement uncertainty in induction machines efficiency estimation," *2014 IEEE International Conference on Power and Energy (PECon)*, 288–292, 2015.
5. Misir, O., S. M. Raziee, N. Hammouche, C. Klaus, R. Kluge, and B. Ponick, "Prediction of losses and efficiency for three-phase induction machines equipped with combined Star-Delta windings," *IEEE Transactions on Industry Applications*, Vol. 53, No. 4, 3579–3587, 2017.
6. Dominguez, J. R., C. Mora-Soto, S. Ortega-Cisneros, J. J. R. Panduro, and A. G. Loukianov, "Copper and core loss minimization for induction motors using high-order sliding-mode control," *IEEE Transactions on Industrial Electronics*, Vol. 59, No. 7, 2877–2889, 2012.
7. Gmyrek, Z., A. Boglietti, and A. Cavagnino, "Estimation of iron losses in induction motors: Calculation method, results, and analysis," *IEEE Transactions on Industrial Electronics*, Vol. 57, No. 1, 161–171, 2010.
8. Roy, R., K. K. Prabhakar, and P. Kumar, "Core-loss calculation in different parts of induction motor," *IET Electric Power Applications*, Vol. 11, No. 9, 1664–1674, 2017.
9. Dems, M. and K. Komeza, "The influence of electrical sheet on the core losses at no-load and full-load of small power induction motors," *IEEE Transactions on Industrial Electronics*, Vol. 64, No. 3, 2433–2442, 2017.
10. Liang, Y., X. Bian, H. Yu, and C. Li, "Finite-element evaluation and eddy-current loss decrease in stator end metallic parts of a large double-canned induction motor," *IEEE Transactions on Industrial Electronics*, Vol. 62, No. 11, 6779–6785, 2015.
11. Yamazaki, K. and W. Fukushima, "Loss analysis of induction motors by considering shrink fitting of stator housings," *IEEE Transactions on Magnetics*, Vol. 51, No. 3, 2015.
12. Cheaytani, J., A. Benabou, A. Tounzi, M. Dessoude, L. Chevallier, and T. Henneron, "End-region leakage fluxes and losses analysis of cage induction motors using 3-D finite-element method," *IEEE Transactions on Magnetics*, Vol. 51, No. 3, 2015.
13. Liang, Y.-P., Y.-L. Hu, X. Liu, and C.-X. Li, "Calculation and analysis of can losses of canned induction motor," *IEEE Transactions on Industrial Electronics*, Vol. 61, No. 9, 4531–4538, 2014.
14. Abshinova, M., "Factors affecting magnetic properties of Fe-Si-Al and Ni-Fe-Mo alloys," *Procedia Engineering*, Vol. 76, 35–44, 2014.
15. O'Handley, R. C., *Modern Magnetic Materials: Principles and Investigations*, Wiley Interscience, 2000.



16. Mc Currie, R. A., *Ferromagnetic Materials Structure and Properties*, Academic Press, 1994.
17. Shirakata, Y., N. Hidaka, M. Ishitsuka, A. Teramoto, and T. Ohmi, "High permeability and low loss Ni-Fe composite material for high-frequency applications," *IEEE Transactions on Magnetics*, Vol. 44, No. 9, 2100–2106, 2008.